ELSEVIER

Journal of Organometallic Chemistry 514 (1996) 73–79

Journal of Organometallic Chemistry

Synthesis and X-ray crystal structures of alkaline-earth metallocenes with pendant substituents

Melanie L. Hays [a], Timothy P. Hanusa [a,*], Terence A. Nile [b]

[a] *Department of Chemistry, Vanderbilt University, Nashville, TN 37235, USA*
[b] *Department of Chemistry, University of North Carolina–Greensboro, Greensboro, NC 27412, USA*

Received 27 July 1995; in revised form 12 October 1995

Abstract

Deprotonation of $[(2\text{-}C_5H_4N)CH_2CMe_2]C_5H_5$ (= HCp^{py}) and $CH_3OCH_2CH_2C_5H_5$ (= $HCp^{\S}$) with $Ae[N(SiMe_3)_2]_2$ (Ae = Ca, Sr, Ba) in toluene produces the corresponding metallocenes, Cp'_2Ae, in high yield. ^1H NMR data reveal that the calcium complex $(Cp^{py})_2Ca$ does not bind tetrahydrofuran. The solid state structures of $(Cp^{py})_2Sr$ and $(Cp^{\S})_2Ca$ were obtained by single crystal X-ray analysis, and found to be monomeric, with the Lewis base substituents on the cyclopentadienyl rings coordinated to the metal centers. Crystals of $(Cp^{py})_2Sr$ grown from toluene are orthorhombic, space group *Pbcn*, with $a = 11.988(4)$ Å, $b = 16.141(4)$ Å, $c = 12.572(4)$ Å, $V = 2433(1)$ Å^3, $Z = 4$, $R = 0.038$, $R_w = 0.043$ based on 635 observed reflections. The complex possesses a bent metallocene geometry and contains a crystallographically imposed two-fold rotation axis passing through the strontium. The average Sr–C and Sr–N distances are 2.85(1) and 2.660(7) Å respectively, and the ring centroid–Sr–ring centroid angle is 141.1°. Crystals of $(Cp^{\S})_2Ca$ grown from toluene are monoclinic, space group $P2_1/n$, with $a = 6.912(4)$ Å, $b = 15.114(2)$ Å, $c = 15.435(3)$, $\beta = 100.34(2)°$, $V = 1586.3(9)$ Å^3, $Z = 4$, $R = 0.041$, $R_w = 0.048$ based on 1318 observed reflections. The complex also has a bent metallocene geometry, with average Ca–C and Ca–O distances are 2.670(6) and 2.407(3) Å respectively; the ring centroid–Ca–ring centroid angle is 136.6°.

Keywords: Calcium; Strontium; Barium; Metallocene; Pendant bases; Crystal structure

1. Introduction

Organoalkaline-earth chemistry has expanded rapidly during the past decade, with its growth dominated by complexes that contain sterically bulky cyclopentadienyl rings [1,2]. The use of such ligands substantially improves both the solubility and volatility of their associated compounds. Alkane-soluble Cp^*_2Ca ($Cp^* = C_5Me_5$), for example, is monomeric in the solid state and sublimes at 75°C, 10^{-3} Torr [3,4], whereas the parent $(C_5H_5)_2Ca$ metallocene is an ether-insoluble, polymeric species that requires 265°C and high vacuum for sublimation [5].

An alternative approach to generating monomeric metallocenes of the heavy Group 2 elements involves the substitution of one position on the cyclopentadienyl ring with a group containing a Lewis base (usually an oxygen or nitrogen donor). Such pendant groups can coordinate intramolecularly to the metal center, so that even when the steric bulk of the pendant group is not large, soluble monomeric complexes can form. The internal coordination of the pendant group can also prevent alkaline-earth metallocenes from forming adducts with solvents that might act as Lewis bases.

Although pendant groups on cyclopentadienyl rings have been successfully used to create monomeric organolanthanide complexes [6,7], few organoalkaline-earth examples are known, and none has been completely characterized. $(\eta^5:\eta^1\text{-}C_5Me_4CH_2CH_2NMe_2)_2Ca$, a colorless solid that sublimes at 110°C, 5×10^{-3} Torr, has been synthesized by the reaction of the substituted potassium cyclopentadienide with CaI_2 in tetrahydrofuran (THF), and by the reaction of the cyclopentadiene and $Ca(NH_2)_2$ in liquid ammonia [8]. Its crystal structure has not been completely solved, but it does confirm the existence of intramolecular coordination. The compound does not form an adduct with THF. Another alkaline-earth metallocene, $Ba(C_5H_4CH_2CH_2OCH_2CH_2OCH_3)_2$, has been synthesized by halide metathesis and by metallation; ^{13}C NMR studies of the

* Corresponding author.

SSDI 0022-328X(95)06015-4

compound suggest that all four oxygen atoms are intramolecularly coordinated [9].

As part of our studies of organoalkaline-earth chemistry [10–13], we sought to develop a synthetic approach to metallocenes with pendant groups that could be used with all three of the heavier metals (Ca–Ba), and that would be applicable to a range of cyclopentadienyl derivatives. The syntheses described here are based on a method that we have successfully used to form octaphenylbarocene [13].

2. Experimental details

2.1. General considerations

All manipulations were performed with the rigid exclusion of air and moisture using high vacuum, Schlenk, or dry box techniques. Proton and carbon (^{13}C) NMR spectra were obtained on a Bruker NR-300 spectrometer at 300 MHz and 75.5 MHz respectively, and were referenced to the residual proton and ^{13}C resonances of THF-d_8 (δ 3.58). Assignments in the ^1H (^{13}C) NMR spectra were made with the help of NOE (DEPT) pulse experiments. Infrared data were obtained on a Perkin–Elmer 1600 Series FT-IR spectrometer. Elemental analyses were performed by Oneida Research Services, Whitesboro, NY. Consistent analyses were difficult to obtain for several complexes; such discrepancies may reflect the extremely air- and moisture-sensitive nature of the compounds. The difficulty in obtaining accurate combustion analyses seems endemic to several types of alkaline-earth compound [14–17].

2.2. Materials

$Ca[N(SiMe_3)_2]_2$ [18], $Sr[N(SiMe_3)_2]_2$ [19], and $Ba[N(SiMe_3)_2]_2$ [20] were prepared using literature procedures. $CH_3OCH_2CH_2C_5H_5$ (= HCp^R), a colorless oil, was prepared from the reaction of $CH_3C_6H_4SO_3CHCH_2OCH_3$ and NaCp in THF, a method similar to one previously reported [21]; however, the reaction mixture was not refluxed under argon, but stirred at room temperature under nitrogen for 18 h. The vacuum-distilled diene was degassed using freeze–pump–thaw cycles and dried over molecular sieves. $[(2\text{-}C_5H_4N)CH_2CMe_2]C_5H_5$ (= HCp^{py}), a light yellow oil, was prepared by a known procedure [22], vacuum distilled, degassed and dried over molecular sieves. Solvents for reactions were distilled under nitrogen from sodium or potassium benzophenone ketyl. THF-d_8 was vacuum distilled from Na–K (22:78) alloy and stored over 4A molecular sieves. All the metallocenes were formed from the reaction of a somewhat greater than 2:1 ratio of the appropriate cyclopentadiene with the alkaline-earth bis(trimethylsilyl)amido compounds. Details are given for the preparation of $(Cp^{py})_2Ca$; except where noted, the other metallocenes were formed similarly.

2.3. Synthesis of $(Cp^{py})_2Ca$

$Ca[N(SiMe_3)_2]_2$ (0.233 g, 0.646 mmol) was dissolved in 20 ml of toluene in an Erlenmeyer flask. To this was added HCp^{py} (0.320 g, 1.61 mmol) with a pipette. The solution was then stirred for 18 h, during which time a solid precipitated. After the reaction mixture was filtered, the retained solid was washed with hexane. The solid was dried under vacuum, leaving $(Cp^{py})_2Ca$ (0.219 g, 78% yield) as a white solid, m.p. 261–263°C. Anal. Found: C, 72.22; H, 7.09; N, 5.77. $C_{28}H_{32}CaN_2$. Calc.: C, 77.02; H, 7.39; N, 6.42%. ^1H NMR (d_8-THF) δ 8.11 (d, $J = 6.0$ Hz, 2H, *o*-py); 7.80 (m, 2H, *p*-py); 7.37 (d, $J = 9.0$ Hz, 2H, *m'*-py); 7.19 (m, 2H, *m*-py); 5.64 and 5.54 (s, 4H, ring-C*H*); 3.05 (s, 4H, CH_2); 1.19 (s, 12H, CH_3). ^{13}C NMR (d_8-THF) δ 162.7 (*o'*-py); 148.8 (*o*-py); 138.9 (*p*-py); 131.8 (ring-*C*C(Me)$_2$CH$_2$py); 128.1 (*m'*-py); 122.1 (*m*-py); 107.0 and 104.4 (ring-*C*H); 54.9 (*C*(Me)$_2$CH$_2$py); 36.3 (*C*H$_2$); 31.1 (*C*H$_3$). Principal IR bands (KBr, cm^{-1}): 3066 (w), 2963 (s), 1592 (m), 1467 (m), 1425 (m).

2.4. Synthesis of $(Cp^{py})_2Sr$

$(Cp^{py})_2Sr$ was isolated in 75% yield as a white solid, m.p. 211–214°C (dec.). The crystal used for X-ray analysis was grown from toluene. Anal. Found: C, 68.09; H, 6.70; N, 5.44. $C_{28}H_{32}N_2Sr$. Calc.: C, 69.46; H, 6.66; N, 5.79%. ^1H NMR (d_8-THF) δ 8.28 (d, $J = 4.5$ Hz, 2H, *o*-py); 7.51 (m, 2H, *p*-py); 7.06 (d, $J = 6.0$ Hz, 2H, *m'*-py); 7.01 (m, 2H, *m*-py); 5.41 and 5.24 (2s, 8H, ring-C*H*); 2.84 (s, 4H, CH_2); 1.21 (s, 12H, CH_3). ^{13}C NMR (d_8-THF) δ 162.5 (*o'*-py); 148.7 (*o*-py); 135.7 (*p*-py); 139.0 (ring-*C*C(Me)$_2$CH$_2$py); 126.0 (*m'*-py); 121.0 (*m*-py); 103.6 and 102.6 (ring-*C*H); 55.7 (*C*(Me)$_2$CH$_2$py); 36.9 (*C*H$_2$); 31.7 (*C*H$_3$). Principal IR bands (KBr, cm^{-1}): 3054 (w), 2957 (s), 1592 (m), 1475 (m), 1430 (m), 1044 (w).

2.5. Synthesis of $(Cp^{py})_2Ba$

An oily layer formed during the reaction; afterwards, the solvent was decanted from the oil, which was then washed with 10 ml hexane. The hexane was decanted, and the oil was placed under vacuum, leaving $(Cp^{py})_2Ba$ (94% yield) as a light tan solid, m.p. 126–127°C (dec.). Anal. Found: C, 66.97; H, 6.67; N, 4.65; Ba, 23.90. $C_{28}H_{32}N_2Ba$. Calc.: C, 62.99; H, 6.04; N, 5.25; Ba, 25.72. ^1H NMR (d_8-THF) δ 8.39 (d, $J = 3.0$ Hz, 2H, *o*-py); 7.52 (m, 2H, *p*-py); 7.06 (m, 2H, *m*-py); 6.96 (d, $J = 9.0$ Hz, 2H, *m'*-py); 5.52 and 5.38 (s, 4H, ring-C*H*);

2.90 (s, 4H, CH_2); 1.24 (s, 12H, CH_3). ^{13} NMR (d_8–THF) δ 162.4 (*o'*-py); 148.7 (*o*-py); 136.1 (*p*-py); 131.1 (ring-$CC(Me)_2CH_2$py); 126.4 (*m*-py); 121.2 (*m'*-py); 106.2 and 105.8 (ring-*C*H); 55.4 ($C(Me)_2CH_2$py); 36.8 (CH_2); 31.3 (CH_3). Principal IR bands (KBr, cm^{-1}): 3065 (w), 2956 (s), 1594 (m), 1436(m), 1058 (m).

2.6. Synthesis of $(Cp^{\S})_2Ca$

A crystalline solid formed during the reaction; it was washed with hexane, then dried under vacuum, leaving $(Cp^{\S})_2Ca$ (64% yield) as small pale yellow crystals, m.p. 139–140°C. These were suitable for X-ray analysis. Anal. Found: C, 67.10; H, 7.80; Ca, 13.66. $C_{16}H_{22}CaO_2$. Calc. C, 67.09; H, 7.74; Ca, 13.99. ^{1}H NMR (d_8–THF) δ 5.65 and 5.56 (m, 4H, ring-C*H*); 3.70 (t, $J = 7.5$ Hz, 4H, CH_2OMe); 3.36 (s, 6H, OCH_3); 2.66 (t, $J = 6.0$ Hz, 4H, CH_2CH_2OMe). ^{13}C NMR (d_8–THF) δ 119.28 (ring-CCH_2CH_2OMe); 106.7 and 105.6 (ring-*C*H); 77.0 (CH_2OMe); 60.1 (OCH_3); 30.7 (CH_2). Principal IR bands (KBr, cm^{-1}): 2953 (s), 2926 (s), 2871 (s), 1608 (s), 1458 (m), 1450 (m), 1458 (m), 1113 (m), 1091 (m).

2.7. Synthesis of $(Cp^{\S})_2Sr$

$(Cp^{\S})_2Sr$ was isolated in 63% yield as an off-white solid, m.p. 113–116°C. Anal. Found: C, 53.32; H, 6.36. $(Cp^{\S})_2Sr$. Calc.: C, 57.54; H, 6.64. ^{1}H NMR (d_8–THF) δ 5.46 and 5.41 (2m, 8H, ring-C*H*); 3.54 (t, $J = 6.0$ Hz, 4H, CH_2OMe); 3.29 (s, 6H, OCH_3); 2.67 (t, $J = 6.0$ Hz, 4H, CH_2CH_2OMe). ^{13}C NMR (d_8–THF) δ 118.3 (ring-CCH_2CH_2OMe); 105.5 and 105.1 (ring-*C*H); 76.8 (CH_2OMe); 58.6 (OCH_3); 31.43 (CH_2). Principal IR bands (KBr, cm^{-1}): 2953 (s), 2926 (s), 2871 (s), 1594 (m), 1458 (m), 1250 (m), 1182 (w), 1115 (m), 932 (w).

2.8. Synthesis of $(Cp^{\S})_2Ba$

$(Cp^{\S})_2Ba$ was isolated in 81% yield as a white solid, m.p. 248–251°C. Anal. Found: C, 52.02; H, 5.91. $(Cp^{\S})_2Ba$. Calc.: C, 50.09; H, 5.78. ^{1}H NMR (d_8–THF) δ 5.48 and 5.46 (2m, 8H, ring-C*H*); 3.63 (t, $J = 6.0$ Hz, 4H, CH_2OMe); 3.39 (s, 6H, OCH_3); 2.67 (t, $J = 6.0$ Hz, 4H, CH_2CH_2OMe). ^{13}C NMR (d_8–THF) δ 122 (ring-CCH_2CH_2OMe); 107.2 and 106.9 (ring-*C*H); 76.9 (CH_2OMe); 59.2 (OCH_3); 31.3 (CH_2). Principal IR bands (KBr, cm^{-1}): 2928 (s), 2864 (s), 1626 (m), 1569 (m), 1447 (m), 1107 (s), 795 (w), 670 (w), 458 (w).

2.9. X-ray crystallography of $(Cp^{py})_2Sr$

A suitable crystal was located and sealed in a glass capillary tube. All measurements were performed on a Rigaku AFC6S diffractometer at Vanderbilt University

Table 1
Crystal data and summary of X-ray data collection for $(Cp^{py})_2Sr$ and $(Cp^{\S})_2Ca$

Compound	$[[2\text{-}(2\text{-}C_5H_4N)CH_2C(Me)_2]C_5H_4]_2Sr$	$(CH_3OCH_2CH_2C_5H_4)_2Ca$
Formula	$C_{28}H_{32}N_2Sr$	$C_{16}H_{22}CaO_2$
Formula weight	484.20	286.43
Color of crystal	colorless	pale yellow
Crystal dimensions (mm^3)	0.19 × 0.23 × 0.13	0.45 × 0.28 × 0.23
Space group	*Pbcn*	$P2_1/n$
Temperature (°C)	20	20
a (Å)	11.988(4)	6.912(4)
b (Å)	16.141(4)	15.114(2)
c (Å)	12.572(4)	15.435(3)
β (deg)		100.34(2)
V (Å^3)	2433(1)	1586.3(9)
Z	4	4
D (calcd) (g cm^{-3})	1.332	1.199
Abs coeff (cm^{-1})	32.04	33.7
Scan speed (deg min^{-1})	2.0	2.0
Scan width	1.31 + 0.30 tan θ	1.37 + 0.30 tan θ
Limits of data collection	6° ≤ 2θ ≤ 120°	6° ≤ 2θ ≤ 120°
Total reflections	2094	2811
Unique reflections	2094	2467
No. with $I > n\sigma(I)$	635 ($n = 2.0$)	1318 ($n = 3.0$)
R(*F*)	0.038	0.041
$R_w(F)$	0.043	0.048
Goodness of fit	1.22	1.61
Max Δ/σ in final cycle	0.01	0.13
Max/min peak (final diff map) (e$^-$ Å^{-3})	0.31/−0.29	0.20/0.15

with graphite monochromated Cu Kα radiation (λ = 1.54178 Å). Relevant crystal and data collection parameters for the present study are given in Table 1.

Sets of diffraction maxima corresponding to an orthorhombic cell were found from a systematic search of a limited hemisphere of reciprocal space; the space group *Pbcn* was uniquely determined from systematic absences. Subsequent solution and refinement of the structure were consistent with the choice.

Data collection was performed using continuous ω–2θ scans with stationary backgrounds (peak:bkgd counting time, 2:1). Data were reduced to a unique set of intensities and associated sigma values in the usual manner. There was no decay in standards, but psi-scans of several representative absorptions indicated a need for an absorption correction. A semiempirical absorption correction was applied with the program DIFABS. The strontium atom was located with Patterson methods and the structure expanded using DIRDIF and Fourier techniques. The asymmetric unit consisted of half the molecule related to the other half by a two-fold rotation axis through the strontium. All non-hydrogen atoms, except the carbon atoms in the pyridyl ring, were refined anisotropically. To improve the refinement of the non-hydrogen atoms, hydrogen atoms were inserted in calculated positions based on packing considerations and d(C–H) = 0.95 Å. The positions were fixed for the final cycles of refinement. A final difference map was featureless. Fractional coordinates and isotropic thermal parameters for the non-hydrogen atoms are listed in Table 2; selected bond distances and angles are listed in Table 3.

Table 2
Fractional coordinates and isotropic thermal parameters

Atom	x	y	z	B_{eq} (Å^2)
$(Cp^{py})_2Sr$				
Sr(1)	0	0.2483(1)	1/4	3.95(5)
N(1)	0.003(1)	0.3598(4)	0.0942(6)	3.7(4)
C(1)	−0.0637(8)	0.3458(4)	0.012(1)	3.9(3)
C(2)	0.6972(5)	0.2163(4)	0.4702(5)	4.8(3)
C(3)	0.054(1)	0.4194(7)	−0.105(1)	4.4(3)
C(4)	0.1247(8)	0.4352(7)	−0.023(1)	4.3(2)
C(5)	0.0992(9)	0.4035(6)	0.0755(9)	3.4(2)
C(6)	0.1775(9)	0.4158(6)	0.1679(8)	3.6(5)
C(7)	0.2723(8)	0.3551(7)	0.182(1)	3.7(6)
C(8)	0.354(1)	0.3609(8)	0.0865(9)	5.0(7)
C(9)	0.336(1)	0.3778(8)	0.2839(9)	5.4(7)
C(10)	0.231(1)	0.2650(7)	0.190(1)	3.6(7)
C(11)	0.1809(9)	0.2185(6)	0.1084(9)	3.5(5)
C(12)	0.150(1)	0.1403(7)	0.147(1)	4.6(7)
C(13)	0.1831(8)	0.1381(6)	0.257(1)	4.6(6)
C(14)	0.230(1)	0.2145(9)	0.282(1)	4.3(7)
$(Cp^{8})_2Ca$				
Ca(1)	0.3759(1)	0.14644(5)	0.17097(6)	4.35(4)
O(1)	0.5930(5)	0.2727(2)	0.1880(2)	5.6(2)
O(2)	0.3276(6)	0.1694(2)	0.3196(2)	6.1(2)
C(1)	0.258(1)	0.1891(5)	0.0052(4)	7.1(4)
C(2)	0.103(1)	0.1418(5)	0.0243(5)	8.0(4)
C(3)	0.016(1)	0.1923(5)	0.0822(5)	7.3(4)
C(4)	0.119(1)	0.2697(4)	0.0981(4)	5.7(3)
C(5)	0.2685(8)	0.2691(4)	0.0495(3)	5.6(3)
C(6)	0.429(1)	0.3364(5)	0.0542(5)	9.8(4)
C(7)	0.562(1)	0.3440(4)	0.1303(5)	10.6(4)
C(8)	0.718(1)	0.2915(5)	0.2678(4)	9.3(4)
C(9)	0.376(1)	−0.0228(3)	0.2176(4)	6.3(3)
C(10)	0.438(1)	−0.0252(4)	0.1373(4)	7.0(4)
C(11)	0.621(1)	0.0123(4)	0.1472(5)	7.4(4)
C(12)	0.676(1)	0.0395(4)	0.2343(6)	7.6(4)
C(13)	0.520(1)	0.0170(3)	0.2785(3)	6.2(3)
C(14)	0.513(1)	0.0407(4)	0.3721(4)	10.7(5)
C(15)	0.360(1)	0.1021(5)	0.3851(4)	9.6(4)
C(16)	0.254(1)	0.2477(5)	0.3497(5)	8.1(4)

$B_{eq} = 8\pi^2/3\Sigma_{i=1}^{3}\Sigma_{j=1}^{3}U_{ij}a_i^* a_j^* \vec{a}_i \cdot \vec{a}_j$

Table 3
Selected bond lengths (Å) and angles (deg) for $(Cp^{py})_2Sr$

Atoms	Distance	Atoms	Angle
Sr–N(1)	2.660(7)	N(1)–Sr–N(1)′	94.9(3)
Sr–C(10)	2.89(1)	N(1)–Sr–C(10)	74.2(3)
Sr–C(11)	2.85(1)	N(1)–Sr–C(10)′	98.4(3)
Sr–C(12)	2.82(1)	Sr–N(1)–C(5)	119.2(7)
Sr–C(13)	2.83(1)	C(5)–C(6)–C(7)	118.2(9)
Sr–C(14)	2.84(1)	C(6)–C(7)–C(8)	110(1)
N(1)–C(1)	1.33(1)	C(8)–C(7)–C(9)	108.4(8)
N(1)–C(5)	1.37(1)	ring centroid–Sr–ring centroid	141.1
C(5)–C(6)	1.51(1)	planarity of rings	within 0.012 Å
C(6)–C(7)	1.51(1)		
C(7)–C(10)	1.54(1)		
C(7)–C(8)	1.55(1)		
C(7)–C(9)	1.54(1)		

2.10. X-ray crystallography of $(Cp^{8})_2Ca$

A suitable crystal was found and sealed in a quartz capillary tube. The general procedure followed was the same as for $(Cp^{py})_2Sr$. Relevant crystal and data collection parameters for the present study are given in Table 1. Cell constants and orientation matrices for data collection were obtained from sets of diffraction maxima corresponding to a monoclinic cell; the space group $P2_1/n$ was uniquely determined from systematic absences.

The data collection and reduction were the same as for $(Cp^{py})_2Sr$. There was no decay in standards, but a semiempirical absorption correction was applied with the program DIFABS. The calcium atom was located with Patterson methods and the structure expanded using DIRDIF and Fourier techniques. All non-hydrogen atoms were refined anisotropically. The hydrogen atoms were inserted in calculated positions based on packing considerations and d(C–H) = 0.95 Å. Their positions were fixed for the final cycles of refinement. A final difference map was featureless. Fractional coordinates and isotropic thermal parameters for the non-hydrogen atoms

Table 4
Selected bond lengths (Å) and angles (deg) for $(Cp^{\S})_2Ca$

Atoms	Distance	Atoms	Angle
Ca(1)–O(1)	2.412(3)	O(1)–Ca(1)–O(2)	88.4(1)
Ca(1)–O(2)	2.401(3)	Ca(1)–O(1)–C(8)	122.0(3)
Ca(1)–C(1)	2.622(6)	Ca(1)–O(2)–C(16)	124.1(4)
Ca(1)–C(2)	2.676(6)	Ca(1)–O(1)–C(7)	121.6(3)
Ca(1)–C(3)	2.705(7)	Ca(1)–O(2)–C(15)	123.0(3)
Ca(1)–C(4)	2.677(6)	C(7)–O(1)–C(8)	113.8(5)
Ca(1)–C(5)	2.646(5)	C(15)–O(2)–C(16)	112.8(5)
Ca(1)–C(9)	2.658(5)	C(5)–C(6)–C(7)	118.6(5)
Ca(1)–C(10)	2.695(6)	C(12)–C(13)–C(14)	124.6(7)
Ca(1)–C(11)	2.710(6)	C(6)–C(7)–O(1)	119.3(6)
Ca(1)–C(12)	2.672(6)	C(14)–C(15)–O(2)	112.6(5)
Ca(1)–C(13)	2.643(5)	C(1)–C(2)–C(3)	107.3(7)
O(1)–C(7)	1.390(6)	C(9)–C(10)–C(11)	108.4(7)
O(1)–C(8)	1.400(6)	ring centroid–Ca–ring centroid	136.6
O(2)–C(15)	1.423(7)	planarity of rings	within 0.007 Å
O(2)–C(16)	1.399(7)		

are listed in Table 2; selected bond distances and angles are listed in Table 4.

3. Results and discussion

3.1. Synthesis and properties of the metallocenes

Initial attempts to synthesize alkaline-earth metallocenes with pendant substituents by metathetical routes (e.g. Eq. (1)) met with limited success. Metallocenes were formed, but were not cleanly isolable owing to the similar solubilities of the desired product and the lithium iodide by-product. Attempts at purification by sublimation were not successful.

$$2LiCp' + AeI_2 \xrightarrow{THF} Cp'_2Ae + 2LiI \ (Ae = Ca, Sr, Ba) \quad (1)$$

In contrast, the metallocenes were readily synthesized in toluene by the reaction of the alkaline-earth bis(amido) complexes with the substituted dienes (Eq. (2)).

$$Ae[N(SiMe_3)_2]_2 + 2HCp' \xrightarrow{toluene} Cp'_2Ae + 2HN(SiMe_3)_2 \quad (2)$$

The volatile amine was removed under vacuum, and washing the alkane-insoluble metallocenes with hexane removed any remaining impurities. The $(Cp^{py})_2Ae$ complexes were more soluble in THF than the $(Cp^{\S})_2Ae$ metallocenes, and for both series, solubility decreased in the order Ca > Sr > Ba. Only $(Cp^{py})_2Sr$ and $(Cp^{\S})_2Ca$ provided crystals of sufficient quality for X-ray studies.

Shifts in the ^1H NMR resonances (in d_8–THF) for the pendant groups indicate that they are coordinated to their respective metal centers in all the metallocenes. For example, the hydrogen atom adjacent to the pyridyl nitrogen in the $(Cp^{py})_2Ae$ complexes appears at δ 8.11, 8.28, and 8.39 ppm in the calcium, strontium, and barium metallocenes respectively. Changes in the spectra of the $(Cp^{\S})_2Ae$ metallocenes are also observed; the resonance for the methylene protons next to the oxygen atom is found at δ 3.70, 3.54, and 3.63 ppm in the Ca, Sr, and Ba complexes respectively. The shift in the pyridyl resonances correlates with the increasing size of the metal center, and thus with a greater distance of the protons from the metal. In the $(Cp^{\S})_2Ae$ metallocenes, changes in solution nuclearity may mask a similar trend in chemical shifts.

The coordination of the pendant groups to the metal centers inhibits the binding of solvents that can act as Lewis bases. $(Cp^{\S})_2Ca$ partially binds THF when recrystallized from the solvent, behavior similar to that of $(Cp^{\S})_2Yb$; the latter, however, forms a THF adduct that is stable enough to be crystallographically characterized [6]. Even more striking is the isolation from THF of totally base-free $(Cp^{py})_2Ca$. This inability to bind THF is especially notable when the extreme tenacity of coordinated THF in other calcocenes is considered; for instance, the THF cannot be completely removed from $Cp^*_2Ca(thf)_2$ by sublimation or repeated refluxing in toluene [4]. The difference in solvent binding ability of the two metallocenes $(Cp^{py})_2Ca$ and $(Cp^{\S})_2Ca$ is notable in that it demonstrates how alterations in the pendant substituent of a cyclopentadienyl ring can be used to control the solvation of the associated metallocene.

The pendant groups affect not only the solvation of the metallocenes, but also their physical properties. The melting points of some of the metallocenes are low, compared with other alkaline-earth complexes with unsubstituted or monosubstituted rings of similar molecular weight. For example, $(Cp^{\S})_2Ca$ and $(Cp^{\S})_2Sr$ (286 and 334 g mol^{-1} respectively) both melt below 140°C, whereas $[(^tBu)C_5H_4]_2Ca$ (282 g mol^{-1}) and $[(^tBu)C_5H_4]_2Sr$ (330 g mol^{-1}) melt at 301–304°C and 375–380°C respectively [23].

The reduced melting points suggested that intermolecular interactions have been lowered between the molecules, and their volatility possibly increased. We therefore examined the volatility of some of the compounds by TGA, since alkaline-earth metallocenes have shown promise as MOCVD reagents for metal oxides and halides [24,25]. The TGA of the pendant metallocenes indicates that they do not possess exceptional volatility when compared with alkaline-earth alkoxides [26]; however, like most other alkaline-earth metallocenes [2], the present compounds display high thermal stability. TGA analysis of $(Cp^{py})_2Sr$ (N_2, 10°C min^{-1}), for example, found $T_{50\%} \approx 710$°C with 31% remaining at 875°C; there were no sharp weight losses from room temperature up to 900°C.

3.2. X-ray crystal structure of $(Cp^{py})_2Sr$

The compound crystallizes from toluene as small colorless blocks. It possesses a bent metallocene geometry, with the Cp^{py} rings and the nitrogen atoms of the pendant pyridyls coordinated to the metal center in a distorted tetrahedral geometry. Owing to a crystallographically imposed C_2 axis through the strontium atom, only half the molecule is unique. An ORTEP view of the complete molecule displaying the numbering scheme used in the tables is provided in Fig. 1.

The average Sr–C distance of 2.85(1) Å is indistinguishable from the 2.845(9) Å value observed in $[(^tBu)C_5H_4]_2Sr(thf)_2$ [23], which also has an eight-coordinate metal center. The individual Sr–C distances vary somewhat, with the distance from the metal to the ring carbon bearing the pyridyl substituent (C(10), 2.89(1) Å) slightly longer than the distances on the other side of the ring (C(12), 2.82(1) Å; C(13), 2.83(1) Å). This pattern has been observed before in the related ytterbium complex $(Cp^{py})_2Yb$ [7].

Apparently, the distance of the Cp^{py} rings from the strontium is such that the coordinated pyridyl groups can be accommodated without inducing substantial structural distortions. This is evident in several parameters; for example, the ring centroid–Sr–ring centroid angle of 141.1° in $(Cp^{py})_2Sr$ represents notably less bending than the comparable angles observed in $[(^tBu)C_5H_4]_2Sr(thf)_2$ and $[C_5H_3\text{-}1,3\text{-}(SiMe_3)_2]_2Sr(thf)$ (133.1° and 134° respectively). Evidently, the pyridyl groups exert less steric pressure on the ring angle than do the THF ligands, though the lack of any bulky substituents on the 'closed' side of $(Cp^{py})_2Sr$ would allow the rings to bend back further than they do. The N(1)–Sr–N(1)' angle of 94.9(3)° has closed appreciably from the comparable 100.8(2)° angle in $(Cp^{py})_2Yb$, although it is larger than the 82.5(2)° N(py)–Yb–N(py)' angle observed between the pyridines in $Cp_2^*Yb(py)_2$ [27].

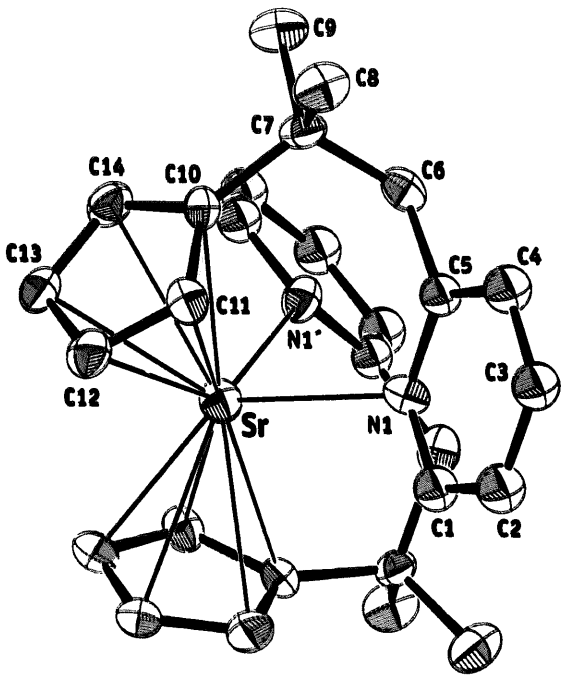

Fig. 1. ORTEP diagram of the non-hydrogen atoms of $(Cp^{py})_2Sr$, illustrating the numbering scheme used in the text. Thermal ellipsoids are shown at the 30% level.

Interpretation of the significance of the Sr–N distance of 2.660(7) Å is not as straightforward. Subtracting the 1.14 Å radius estimated for Sr^{2+} from the Sr–N separation leaves 1.40 Å as the 'effective radius' for the pyridyl nitrogen atom. This value is close to the 1.43 Å effective pyridyl nitrogen radius in $Cp_2^*Yb(py)_2$, but shorter than the 1.52 Å average value for the pyridine nitrogens in (*N*-carbazolyl)$_2$Ca(py)$_4$ [28]. All these values are appreciably larger than the 1.34 Å effective N radius observed in $(Cp^{py})_2Yb$. The latter value implies that the pyridyls are held relatively more closely to the metal center in $(Cp^{py})_2Yb$ than in $(Cp^{py})_2Sr$; this may be a consequence of conformational changes forced on the ligand by trying to bond to the smaller ytterbium center.

3.3. X-ray crystal structure of $(Cp^{\$})_2Ca$

The complex crystallizes from toluene as small pale yellow prisms. Like $(Cp^{py})_2Sr$, it possesses a bent metallocene geometry, with the $Cp^{\$}$ rings and the oxygen atoms of the pendant methoxyethyl substituents coordinated to the metal center in a distorted tetrahedral geometry. The molecule has approximate C_2 symmetry, although it is not crystallographically imposed. An ORTEP view of the complete molecule displaying the numbering scheme used in the tables is provided in Fig. 2

The average Ca–C distance of 2.670(6) Å in $(Cp^{\$})_2Ca$ is indistinguishable from the 2.676(9) Å value observed in the eight-coordinate $(MeCp)_2Ca(dme)$ [29], although it is slightly shorter than the Ca–C distance in $[(^tBu)C_5H_4]_2Ca(thf)$ (2.733 Å) [23]. Unlike the pattern of M–C bond lengths observed in $(Cp^{py})_2Sr$, the ring carbons bearing the pendant substituent in $(Cp^{\$})_2Ca$ have either the shortest or the next to shortest Ca–C distances (Table 4).

The ring centroid–Ca–ring centroid angle of 136.6° in $(Cp^{\$})_2Ca$ does not differ greatly from the angles found in $(MeCp)_2Ca(dme)$, $[(^tBu)C_5H_4]_2Ca(thf)_2$, and $[C_5H_3\text{-}1,3\text{-}(SiMe_3)_2]_2Ca(thf)$ (134.8°, 133.3°, and 135.1° respectively). The O(1)–Ca–O(2) angle of 88.4(1)° is slightly larger than the angle between the THF ligands in $[(^tBu)C_5H_4]_2Ca(thf)_2$ (83.2°) and $[(^tBu)C_5H_4]_2Sr(thf)_2$ (83.1°), although it is substantially greater than the 68.7° angle in O–Ca–O in $(MeCp)_2Ca(dme)$, which is dictated by the bite of the chelating DME.

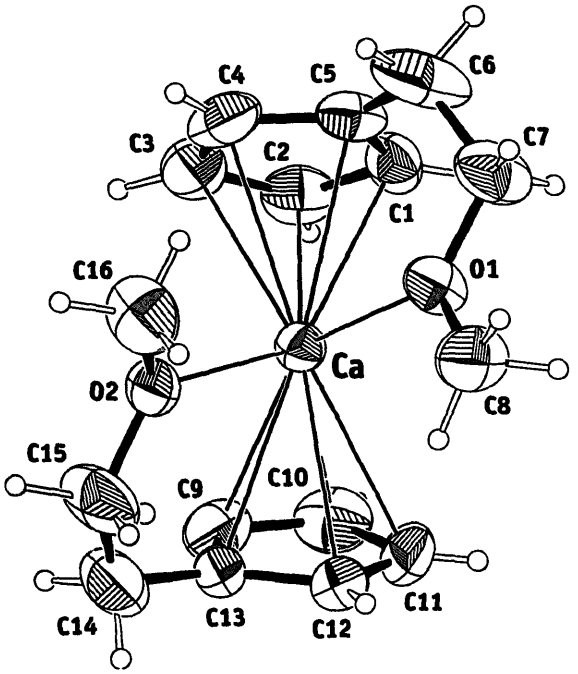

Fig. 2. ORTEP diagram of $(Cp^8)_2Ca$, illustrating the numbering scheme used in the text. Thermal ellipsoids are shown at the 30% level.

The fact that the ether oxygens are held in a chelated ring in $(Cp^8)_2Ca$ does not affect their distance to the metal. The Ca–O distances of 2.412(3) Å and 2.401(3) Å are essentially the same as the Ca–O lengths observed in $[('Bu)C_5H_4]_2Ca(thf)_2$ (2.402 Å), and are comparable with the 2.310(9) Å distance observed in $[C_5H_3\text{-}1,3\text{-}(SiMe_3)_2]_2Ca(thf)$ when the 0.06 Å difference between seven- and eight-coordinate Ca^{2+} is considered [30].

4. Conclusion

Metallocenes are readily formed from the reaction of cyclopentadienes carrying pendant oxygen- or nitrogen-donor Lewis bases with the alkaline-earth bis(trimethylsilyl)amides. The bases coordinate to the metal centers, reducing the tendency of the complexes to coordinate solvent molecules, and ensuring that the metallocenes are monomeric. These complexes demonstrate that control over nuclearity of compounds with the heavier Group 2 metals is possible without recourse to multiply substituted, sterically bulky cyclopentadienyl rings.

Acknowledgments

Acknowledgment is made to the Petroleum Research Fund for support of this research. Funds for the X-ray diffraction facility at Vanderbilt University were provided through NSF Grant CHE-8908065. We thank Dr. Stephen B. Milne for assistance with the TGA measurements.

References

[1] T.P. Hanusa, *Polyhedron, 9* (1990) 1345.
[2] T.P. Hanusa, *Chem. Rev., 93* (1993) 1023.
[3] C.J. Burns and R.A. Andersen, *J. Organomet. Chem., 325* (1987) 31.
[4] R.A. Williams, T.P. Hanusa and J.C. Huffman, *Organometallics, 9* (1990) 1128.
[5] R. Zerger and G. Stucky, *J. Organomet. Chem., 80* (1974) 7.
[6] C. Qian, B. Wang, D. Deng, J. Hu, J. Chen, G. Wu and P. Zheng, *Inorg. Chem., 33* (1994) 3382.
[7] J.R. Van den Hende, P.B. Hitchcock, M.F. Lappert and T.A. Nile, *J. Organomet. Chem., 472* (1994) 79.
[8] P. Jutzi and J. Dahlhaus, *Coord. Chem. Rev., 137* (1994) 179.
[9] W.S. Rees, Jr., U.W. Lay and K.A. Dippel, *J. Organomet. Chem., 483* (1994) 27.
[10] M.J. McCormick, R.A. Williams, L.J. Levine and T.P. Hanusa, *Polyhedron, 7* (1988) 725.
[11] R.A. Williams, K.F. Tesh and T.P. Hanusa, *J. Am. Chem. Soc., 113* (1991) 4843.
[12] D.J. Burkey, R.A. Williams and T.P. Hanusa, *Organometallics, 12* (1993) 1331.
[13] P.S. Tanner and T.P. Hanusa, *Polyhedron, 13* (1994) 2417.
[14] M.J. McCormick, S.C. Sockwell, C.E.H. Davies, T.P. Hanusa and J.C. Huffman, *Organometallics, 8* (1989) 2044.
[15] S.C. Sockwell, T.P. Hanusa and J.C. Huffman, *J. Am. Chem. Soc., 114* (1992) 3393.
[16] B.A. Vaartstra, J.C. Huffman, W.E. Streib and K.G. Caulton, *Inorg. Chem., 30* (1991) 121.
[17] M.G. Gardiner, G.R. Hanson, P.C. Junk, C.L. Raston, B.W. Skelton and A.H. White, *J. Chem. Soc. Chem. Commun.*, (1992) 1154.
[18] P.S. Tanner, D.J. Burkey and T.P. Hanusa, *Polyhedron, 14* (1995) 331.
[19] J.S. Overby and T.P. Hanusa, in preparation.
[20] J.M. Boncella, C.J. Coston and J.K. Commack, *Polyhedron, 10* (1991) 769.
[21] H. Qichen, Q. Yanlong, L. Guisheng and T. Youqi, *Transition Met. Chem., 15* (1990) 483.
[22] B.M. Misquitta, *M.S. Thesis*, University of North Carolina at Greensboro, 1993.
[23] M.G. Gardiner, C.L. Raston and C.H.L. Kennard, *Organometallics, 10* (1991) 3680.
[24] M.J. Benac, A.H. Cowley, R.A. Jones and A.F. Tasch, Jr., *Chem. Mater., 1* (1989) 289.
[25] P.S. Kirlin, D.W. Brown, and R.A. Gardiner. U.S. Patent 5225561, 1993.
[26] S.R. Drake, D.J. Otway, M.B. Hursthouse and K.M. Abdul Malik, *J. Chem. Soc. Dalton Trans.*, (1993) 2883.
[27] T.D. Tilley, R.A. Andersen, B. Spencer and A. Zalkin, *Inorg. Chem., 21* (1982) 2647.
[28] G. Mösges, F. Hampel, M. Kaupp and P.v.R. Schleyer, *J. Am. Chem. Soc., 114* (1992) 10880.
[29] A. Hammel, W. Schwarz and Weidlein, *J. Organomet. Chem., 378* (1989) 347.
[30] R.D. Shannon, *Acta Crystallogr. Sect. A:, 32* (1976) 751.